© 2015. Published by The Company of Biologists Ltd | Journal of Cell Science (2015) 128, 2350-2360 doi:10.1242/jcs.168096

RESEARCH ARTICLE

Negative feedback from CaSR signaling to aquaporin-2 sensitizes vasopressin to extracellular Ca^{2+}

Marianna Ranieri[1,*], Grazia Tamma[1,2,*], Annarita Di Mise[1], Annamaria Russo[1], Mariangela Centrone[1], Maria Svelto[1,2,3], Giuseppe Calamita[1,2] and Giovanna Valenti[1,2,3,‡]

ABSTRACT

We previously described that high luminal Ca^{2+} in the renal collecting duct attenuates short-term vasopressin-induced aquaporin-2 (AQP2) trafficking through activation of the Ca^{2+}-sensing receptor (CaSR). Here, we evaluated AQP2 phosphorylation and permeability, in both renal HEK-293 cells and in the dissected inner medullary collecting duct, in response to specific activation of CaSR with NPS-R568. In CaSR-transfected cells, CaSR activation drastically reduced the basal levels of AQP2 phosphorylation at S256 (AQP2-pS256), thus having an opposite effect to vasopressin action. When forskolin stimulation was performed in the presence of NPS-R568, the increase in AQP2-pS256 and in the osmotic water permeability were prevented. In the freshly isolated inner mouse medullar collecting duct, stimulation with forskolin in the presence of NPS-R568 prevented the increase in AQP2-pS256 and osmotic water permeability. Our data demonstrate that the activation of CaSR in the collecting duct prevents the cAMP-dependent increase in AQP2-pS256 and water permeability, counteracting the short-term vasopressin response. By extension, our results suggest the attractive concept that CaSR expressed in distinct nephron segments exerts a negative feedback on hormones acting through cAMP, conferring high sensitivity of hormone to extracellular Ca^{2+}.

KEY WORDS: AQP2 phosphorylation, Ca^{2+}-sensing receptor, CaSR, Vasopressin

INTRODUCTION

Vasopressin-elicited water reabsorption is mediated by the cAMP-dependent trafficking of vesicles containing the water channel aquaporin-2 (AQP2) into the apical membrane of collecting ducts (Nedvetsky et al., 2009; Wilson et al., 2013). We have previously provided evidence that high concentrations of luminal Ca^{2+} in the renal collecting duct attenuate short-term vasopressin-induced AQP2 trafficking through Ca^{2+}-sensing receptor (CaSR) activation (Procino et al., 2012, 2004, 2008). The data supporting this conclusion were obtained both from *in vitro* experiments using AQP2-expressing mouse collecting duct cells (MCD4 cells) and from hypercalciuric patients (Procino et al., 2012). Specifically, acute CaSR activation by selective agonists reduced AQP2 translocation to the plasma membrane in response to the cAMP-stimulating agent forskolin. Moreover, in hypercalciuric patients, evaluation of renal response to the synthetic vasopressin drug DDAVP demonstrated a moderate urinary concentrating defect in these subjects, paralleled by reduced urinary excretion of AQP2. These findings support the hypothesis that the CaSR–AQP2 interplay represents an internal renal defense to mitigate the effect of hypercalciuria on the risk of Ca^{2+} saturation during antidiuresis as initially suggested by Sands et al. (Sands et al., 1997). Clinical evidence for an effect of luminal Ca^{2+} on AQP2-mediated water reabsorption was provided for the first time in our previous studies in enuretic children (Valenti et al., 2000). Interestingly, hypercalciuric enuretic children treated with a low-Ca^{2+} diet to reduce hypercalciuria had decreased overnight urine output and increased nighttime AQP2 excretion and osmolality (Valenti et al., 2002). More recently, we provided further evidence for the inverse relationship between calciuria and water metabolism in a bed-rest study. Bed-rest induced an increase in blood hematocrit (reflecting water loss), which coincided to a reduction of urinary AQP2 likely paralleled by an increase in urinary Ca^{2+} due to bone demineralization (Tamma et al., 2014a).

Besides the effect on AQP2 trafficking, previous findings demonstrated that high external Ca^{2+} reduces AQP2 expression both in the collecting duct cell line mpkCCD and in hypercalciuric rats (Bustamante et al., 2008; Sands et al., 1998). In humans, vitamin-D-elicited hypercalcemia or hypercalciuria is associated with polyuria. In rats dihydrotachysterol (DHT) induces AQP2 water channel downregulation despite unaltered AQP2 mRNA expression, an effect that has been attributed to activation of the Ca^{2+}-sensitive protease calpain (Puliyanda et al., 2003). Taken together, these data support a direct effect of luminal Ca^{2+} on AQP2 expression in collecting duct principal cells and point to a role of Ca^{2+} in regulating both AQP2 trafficking and expression.

To evaluate whether CaSR activation in renal cells modulates AQP2 trafficking and/or expression by alteration of its phosphorylation state, here, AQP2 phosphorylation and function was analyzed in renal HEK-293 cells stably expressing human AQP2 and transfected with wild-type CaSR (CaSR-wt). To mimic 'tonic' activation of CaSR in collecting duct epithelial cells, HEK cells were also transfected with two gain-of-function variants of CaSR, the CaSR-N124K mutation and the CASR-R990G gene polymorphism. Both these activating CaSR variants predispose humans to nephrolithiasis and have been recently characterized at cellular level (Ranieri et al., 2013). In parallel experiments, AQP2 phosphorylation dynamics in response to the specific CaSR positive allosteric modulator NPS-R568 were evaluated in isolated mouse collecting duct to exclude the contribution of the CaSR highly expressed in the thick ascending limb. Our *in vitro* and *ex vivo* data provide interesting indications that specific activation of CaSR expressed in the collecting duct prevents the cAMP-dependent increase in AQP2 phosphorylation at S256 (AQP2-pS256) and water reabsorption, and point to a crucial role of CaSR signaling in

[1]Dept of Biosciences, Biotechnologies and Biopharmaceutics, University of Bari, Aldo Moro, 70125, Bari, Italy. [2]Istituto Nazionale di Biostrutture e Biosistemi (I.N.B.B.) 00136, Rome, Italy. [3]Centro di Eccellenza di Genomica in campo Biomedico ed Agrario (CEGBA) 70125, Bari, Italy.
*These authors contributed equally to this work

‡Author for correspondence (giovanna.valenti@uniba.it)

Received 23 December 2014; Accepted 5 May 2015

Journal of Cell Science

Journal of Cell Science (2015) 128, 2350-2360 doi:10.1242/jcs.168096

impairing the short-term vasopressin response. The intriguing hypothesis that there is a general physiological role of CaSR expressed in distinct nephron segments as a negative mechanism to counteract hormones acting through the cAMP pathway is discussed.

RESULTS

Expression of CaSR variants alters basal AQP2 phosphorylation, PKA activity and osmotic water permeability in HEK-293 cells

The effect of ectopic expression of human CaSR-wt and its gain-of-function (CaSR-R990G, CaSR-N124K) variants on the basal levels of AQP2 phosphorylation was evaluated in HEK-293 cells using phosphospecific antibodies. Compared to mock cells (stably expressing AQP2 but not CaSR) a significant increase in AQP2-pS256 was observed in CaSR-wt-, CaSR-R990G- and CaSR-N124K-expressing cells (Fig. 1). Similarly, expression of CaSR-wt resulted in a significant increase in AQP2 phosphorylation at S261 (AQP2-pS261) levels, compared to mock cells. Moreover the AQP2-pS261 levels appeared to be significantly higher in cells expressing the gain-of-function variants compared to CaSR-wt-expressing cells (Fig. 1). No significant modification of the AQP2 phosphorylation at T269 (AQP2-pT269) was observed in any of the cells expressing CaSR variants (data not shown).

To evaluate whether the increase in AQP2-pS256 levels coincided with an increase in osmotic water permeability, functional studies were performed. Consistent with the obtained data on AQP2-pS256 levels, a significantly higher osmotic response, as compared to mock cells, was observed in cells expressing CaSR-wt or CaSR-R990G and CaSR-N124K (Fig. 2A). Taken together, these *in vitro* data indicate that ectopic expression of CaSR or its activating variants increases the basal cell permeability by increasing the AQP2-pS256 levels and, hence, the constitutive AQP2 trafficking to the plasma membrane.

Given that AQP2-pS256 is under control of protein kinase A (PKA), fluorescence resonance energy transfer (FRET) experiments were performed to evaluate basal PKA activity in CaSR-expressing cells. Compared to mock cells (stably transfected with AQP2 but not with CaSR), normalized FRET (nFRET) signals were found to be significantly lower in cells expressing CaSR-wt and CaSR-R990G variants, indicating that the basal PKA activity was significantly higher (Fig. 2B). These data are in agreement with the AQP2-pS256 levels found in CaSR-expressing cells. By contrast, a slightly, though significantly, lower basal PKA activity, was found for the CaSR-N124K variant indicating that the increase in basal AQP2-pS256 observed in those cells was instead PKA independent.

The higher PKA activity found in CaSR-wt-expressing cells might be due to a reduced basal activity of protein phosphatase 2A (PP2A), which is known to de-phosphorylate AQP2 in intact cells (Tamma et al., 2014b), or to reduced phosphodiesterase 1 (PDE1) activity, in both cases secondary to the significant reduction of basal intracellular Ca^{2+} upon expression of functional CaSR, as previously shown in HEK-293 cells (Ranieri et al., 2013). Experiments with vinpocetine, a selective inhibitor of the Ca^{2+}-dependent PDE1, showed that, although treatment with vinpocetine significantly increased the osmotic water permeability in mock cells (expressing AQP2 and not CaSR), in cells expressing the CaSR-wt, vinpocetine was ineffective (supplementary material Fig. S1). By contrast, no significant reduction of basal PP2A activity was found in CaSR-wt-expressing cells (data not shown). These findings indicate that PDE1 inhibition is likely responsible for the increase in basal cAMP levels and in PKA activity leading to a higher basal osmotic water permeability.

Specific activation of CaSR with NPS-R568 reduces basal AQP2-pS256 levels

We next evaluated the effect of selective CaSR activation with the positive allosteric modulator NPS-R568 (Nemeth et al., 1996) on AQP2 phosphorylation. NPS-R568 is known for acting selectively on the CaSR (Nemeth et al., 1998). Fig. 3 reports the effect of NPS-R568 on the basal levels of AQP2-pS256 phosphorylation.

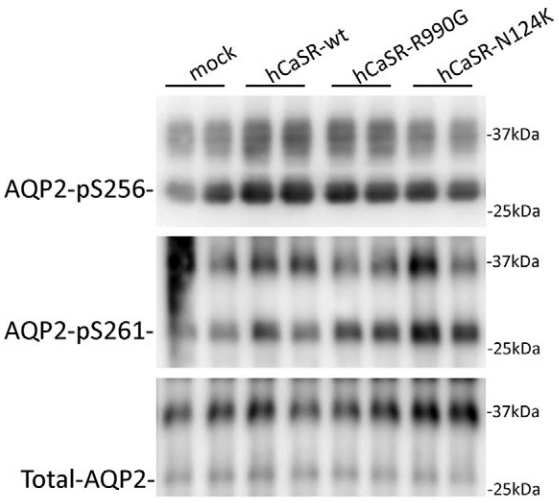

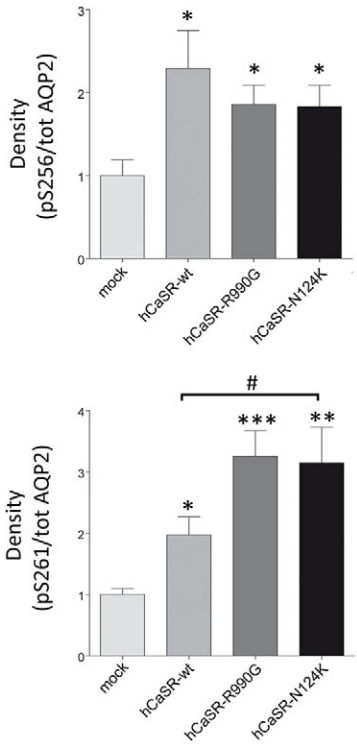

Fig. 1. S256 and S261 phosphorylation of AQP2 in HEK-293 cells. Cells stably expressing AQP2 were transiently transfected with human (h)CaSR-wt and its gain-of-function variants (CaSR-R990G, CaSR-N124K). After transfection cells were subjected to immunoblotting using antibodies against AQP2 phosphorylated at S256 (AQP2-pS256), S261 (AQP2-pS261) or total AQP2 (indicated). Densitometric analysis and statistical studies (mean±s.e.m.) revealed a significant increase of pS256 (n=6) and pS261 (n=9) in cells expressing CaSR-wt and its gain-of-function variants with respect to mock cells. AQP2-pS261 and AQP2-pS256 were normalized against total AQP2, mock conditions were set to 1. *P<0.01, **P<0.001. ***P<0.0001 versus mock; #P<0.001 versus CaSR-wt.

Journal of Cell Science (2015) 128, 2350-2360 doi:10.1242/jcs.168096

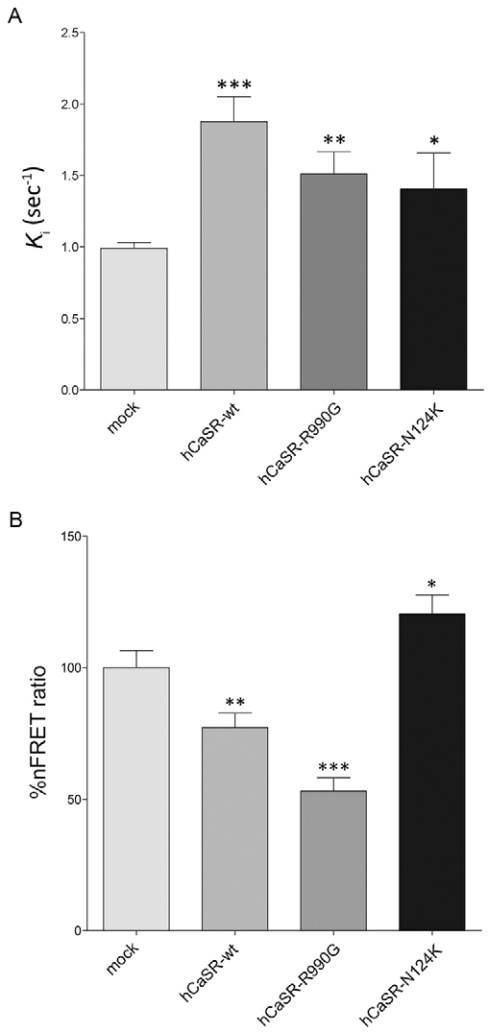

Fig. 2. Osmotic water permeability and PKA activity in HEK-293 cells. (A) Time constant of cell swelling under hypertonic stimulus. Cells were grown and transfected as described in Materials and Methods section and exposed to a hypertonic gradient. The time course of fluorescence changes in cells loaded with Calcein Red-Orange indicates that, compared with mock, cells expressing human (h)CaSR-wt and its gain-of-function variants have a significantly higher basal osmotic water permeability, reported as K_i (mean± s.e.m.; *P<0.01, **P<0.001. ***P<0.0001 versus mock). (B) Evaluation of PKA activity by FRET analysis. The histogram compares the changes of nFRET ratio, among mock and cells expressing CaSR-wt, CaSR-R990G and CaSR-N124K. FRET studies indicate that the steady state PKA activity is significantly higher in CaSR-wt- and CaSR-R990G-expressing cells. By contrast, in cells expressing CaSR-N124K the PKA activity was found to be significantly lower compared to mock (mean± s.e.m.; *P<0.01, **P<0.001, ***P<0.0001 versus mock).

Interestingly, specific activation of CaSR with the allosteric modulator resulted in a strong reduction of the AQP2-pS256 basal levels in all cells expressing CaSR-wt or its activating variants compared to cells not expressing the CaSR. No significant changes in AQP2-pS261 basal levels in response to NPS-R568 were observed in cells expressing CaSR-wt or its gain-of-function variants (Fig. 3).

CaSR signaling prevents the increase in AQP2-pS256 and the osmotic water permeability in response to forskolin through inhibition of cAMP synthesis by the adenylate cyclase

Given that CaSR activation reduces the basal levels of AQP2-pS256, we next evaluated whether CaSR signaling modulates the effect of the cAMP elevating agent forskolin, on AQP2 phosphorylation at S256 and S261. AQP2 phosphorylation was therefore analyzed in renal HEK-293 cells in response to forskolin in the presence or in the absence of the specific activation of CaSR with the positive allosteric modulator NPS-R568. In cells not expressing CaSR but stably expressing AQP2 (mock), forskolin treatment resulted in a strong increase in AQP2-pS256, paralleled by a reduction in AQP2-pS261 (Fig. 4), thus simulating the effect on AQP2 phosphorylation observed after exposure of native collecting duct principal cells to vasopressin (Hoffert et al., 2006). However, when forskolin stimulation was performed in HEK-293 cells expressing CaSR-wt, no significant increase in AQP2-pS256 was found either in the presence or in the absence of NPS-R568. This observation suggests that CaSR signaling impairs the forskolin-dependent increase in AQP2-pS256. In contrast, CaSR expression did not influence the forskolin-induced decrease in AQP2-pS261 regardless of whether NPS-R568 was present. This suggests that in renal cells under forskolin stimulation, hence, simulating vasopressin action, the presence of CaSR counteracts forskolin response mainly through inhibition of AQP2 phosphorylation at S256.

Next, functional studies were carried out. In mock cells stably expressing AQP2 but not CaSR, forskolin stimulation induced a significantly higher temporal osmotic response (reported as K_i, P<0.0001), which, as expected, was not affected by NPS-R568 (Fig. 5A). In contrast, in cells expressing CaSR-wt the increase in K_i was prevented (Fig. 5A). Moreover, when forskolin stimulation was performed in the presence of NPS-R568, the response was significantly reduced with respect to forskolin action alone, suggesting that the signaling associated with CaSR activation contributes significantly to the inhibitory effect of CaSR signaling on forskolin-induced increase in osmotic water permeability (Fig. 5A). This was further confirmed by the observation that the sole exposure of cells to NPS-R568 reduced the osmotic water permeability of CaSR-wt-expressing cells, likely reflecting the observed reduction in basal AQP2-pS256 levels. Of interest, no increase in water permeability was also seen in the cells expressing the CaSR-activating variants exposed to forskolin (data not shown). Taken together, these data indicate that, *in vitro*, the ectopic expression of a functional CaSR and its signaling blunts the osmotic response to the cAMP-elevating agents forskolin. Likely, this occurs mainly through impairments of AQP2 phosphorylation at S256.

In line with those findings, FRET experiments showed that, although in mock cells not expressing CaSR, stimulation with forskolin resulted in a strong activation of PKA (depicted as a reduction of the nFRET signal, Fig. 5B) regardless of the presence of NPS-R568, no significant increase in PKA activity in response to forskolin was observed in CaSR-expressing cells either in the presence or in the absence of NPS-R568. The PKA activity measurements are in agreement with the AQP2-pS256 levels found in each experimental condition and with the functional data.

To evaluate whether, like in native kidney cells, CaSR signaling acts through decreasing adenylyl cyclase activity, the effect of a cell permeable cAMP analog on water permeability was assessed in the absence or presence of NPS-R568. Mock cells (not expressing CaSR and expressing AQP2) and CaSR-wt-expressing cells were treated with the cell permeable cAMP analog 8-Br-cAMP in the absence or in the presence of the NPS-R568. 8-Br-cAMP stimulation resulted in a significant increase in the osmotic water permeability regardless of NPS-R568 treatment in mock and in CaSR-wt cells (Fig. 5C). Given that forskolin stimulation resulted instead in a significant decrease in the osmotic water permeability

Journal of Cell Science (2015) 128, 2350-2360 doi:10.1242/jcs.168096

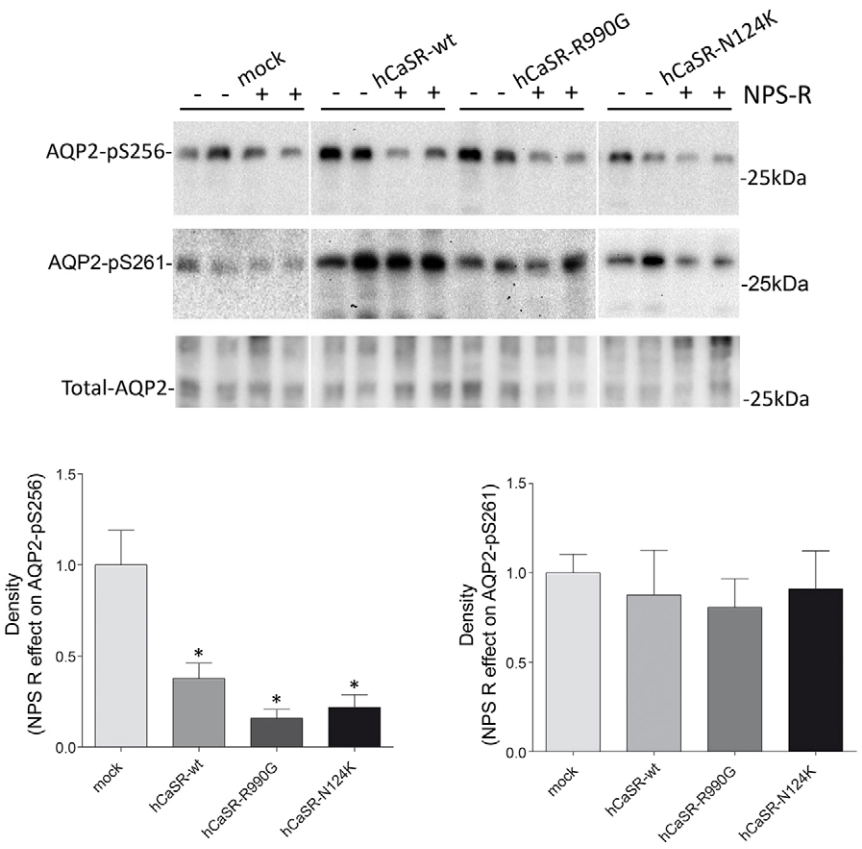

Fig. 3. Effect of NPS-R568 on S256 and S261 phosphorylation of AQP2. Cells expressing human (h)CaSR-wt and its gain-of-function variants (CaSR-R990G, CaSR-N124K) were subjected to immunoblotting using antibodies against AQP2 phosphorylated at S256 (AQP2-pS256), S261 (AQP2-pS261) or total AQP2 (as indicated). Densitometric analysis and statistical studies revealed that NPS-R568 (NPS R) caused a significant decrease in AQP2-pS256 (n=5) in cells expressing CaSR-wt and its gain-of-function variants with respect to mock cells. No effect of NPS-R568 on AQP2-pS261 levels was observed. Histograms compare changes in the ratio of density values of NPS-R568-treated cells with respect to untreated cells. The mock ratio condition was set to 1 (mean±s.e.m.; *P<0.01 versus mock).

under NPS-R568 treatment (Fig. 5A), taken together, these data indicate that CaSR signaling exerts its inhibitory action mostly by reducing the activity of adenylyl cyclase.

CaSR signaling prevents forskolin-induced AQP2-pS256 in isolated mouse collecting duct tubules and in rat kidney inner medulla

Given that the data obtained in HEK-283 renal cells refers to the interplay between the CaSR and the AQP2, both of which are expressed in the collecting duct, the following step was to evaluate the physiological relevance of these data in isolated mouse collecting tubules exposed to forskolin in the presence or in the absence of NPS-R568. These experiments were performed to selectively stimulate CaSR in the collecting duct excluding the proximal tubule and the thick ascending limb, where CaSR is expressed on the luminal and on the basolateral side, respectively (Riccardi and Brown, 2010; Brown, 1999). In freshly dissected collecting duct tubules, forskolin treatment caused a nearly threefold increase in AQP2-pS256 with respect to control (Fig. 6A). Interestingly, and in line with the data obtained in renal cells, forskolin stimulation performed in the presence of NPS-R568 resulted in a complete abrogation of the increase in AQP2-pS256. NPS-R568 alone did not alter the basal level of AQP2-pS256 (Fig. 6A). Conversely, exposure of isolated collecting ducts to forskolin treatment caused a significant decrease in AQP2-pS261 with respect to control. However, simultaneous stimulation of isolated tubules with NPS-R568 and forskolin did not prevent the significant reduction of AQP2-pS261. NPS-R568 alone did not affect the basal levels of AQP2-pS261 (Fig. 6A). In line with western blotting data, immunolocalization of AQP2 in mouse inner medulla confirmed that, although AQP2 relocalized to the apical membrane under forskolin treatment, this effect was prevented in collecting ducts exposed to forskolin in the presence of NPS-R568, a condition in which AQP2 appeared to localize intracellularly (Fig. 6B). Parallel experiments conducted in a mouse collecting duct cell line stably transfected with AQP2 (MCD4) and wt-CaSR confirmed that stimulation with forskolin in the presence of NPS-R568, abrogated AQP2 trafficking to the apical plasma membrane (supplementary material Fig. S2). The effects of forskolin stimulation on AQP2-pS256 and AQP2-pS261 levels in the presence of NPS-R568 were also evaluated in isolated rat kidney inner medulla preparations (inner medulla kidney slices) leading to very similar results. In fact, in rat kidney, the presence of NPS-R568 during forskolin stimulation prevented the increase in AQP2-pS256, whereas it had no effect on the decrease in AQP2-pS261 associated with forskolin treatment (Fig. 7). The expression of CaSR in this sample was confirmed by western blotting using specific antibodies (Fig. 7). Control experiments testing the effect of Ca^{2+} (the physiological CaSR agonist) on AQP2 phosphorylation in inner medulla rat kidney slides, demonstrated that 5 mM Ca^{2+} reproduced the same results obtained using NPS-R568 as CaSR agonist (supplementary material Fig. S3).

CaSR signaling reduces the forskolin-induced increase in water permeability of the mouse collecting duct membrane vesicles as shown by stopped-flow light scattering experiments

Stopped-flow light scattering experiments were carried out to evaluate whether the observed impairment of the forskolin-induced increase in AQP2-pS256 under CaSR activation in isolated mouse collecting duct leads to the reduction of the osmotic water permeability. To do that, plasma membrane vesicles prepared from freshly isolated mouse collecting ducts from 25 sham mice were subjected rapidly (1 ms) to a hypertonic osmotic gradient of 140 mOsm and the resulting time course of vesicle shrinkage was

Journal of Cell Science (2015) 128, 2350-2360 doi:10.1242/jcs.168096

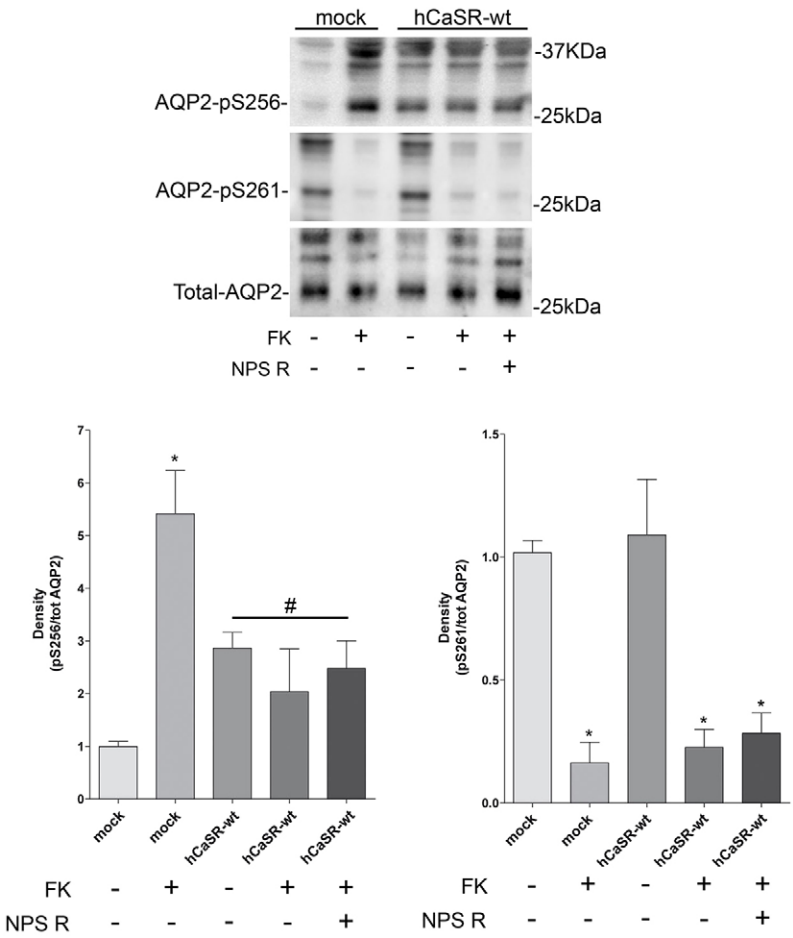

Fig. 4. Effect of NPS-R568 and forskolin on S256 and S261 phosphorylation of AQP2. Mock and cells expressing human (h)CaSR-wt were treated with forskolin (FK) and/or NPS-R568 and subjected to immunoblotting using antibodies against AQP2-pS256, AQP2-pS261 or total AQP2 (as indicated). Compared to mock, in cells expressing CaSR-wt, statistical analysis of data (mean±s.e.m.) revealed that forskolin failed in increasing AQP2-pS256 regardless the presence of NPS-R568 (NPS R) (n=3, *P<0.0001). By contrast, the AQP2-pS256 levels were found significantly lower compared to the maximal AQP2-pS256 levels found in mock cells under forskolin action ($^{\#}P$<0.001 verus forskolin-treated mock cells). NPS-R568 had no effect on AQP2-pS261 in mock and cells expressing CaSR-wt (n=3).

followed by measuring the change in scattered light. The measured K_i values were used to calculate the coefficient of osmotic membrane water permeability (P_f, μm s^{-1}). Consistent with the observed impairment in the increase in AQP2-pS256 in response to forskolin under CaSR activation with NPS-R568, the significant increase in P_f of the vesicles from isolated collecting duct exposed to forskolin was prevented, and was not significantly different from the P_f measured in control vesicles. No significant effect of NPS-R258 alone on P_f was observed (Table 1).

The relatively small increase in P_f measured in vesicles after exposure to forskolin was likely due to the presence, besides AQP2, of AQP4, a water channel highly permeable to water, which would be expected to mask the increase in P_f after forskolin stimulation. Indeed, western blotting analysis of vesicles used in the stopped-flow light scattering study showed expression of both AQP2 and AQP4 (supplementary material Fig. S4). By contrast, no contamination of intracellular membrane was detected (supplementary material Fig. S4). The specific CaSR expression was confirmed by western blotting analysis using specific antibodies detecting both the 120-kDa and the mature glycosylated CaSR form at 160 kDa (supplementary material Fig. S4).

DISCUSSION

The present study shows, both in renal cells and in microdissected collecting duct, that the inhibitory effect of CaSR signaling on AQP2 trafficking to the plasma membrane in response to the cAMP elevating agent forskolin is mainly due to a strong reduction in AQP2 phopshorylation at S256, resulting in severe impairment of the osmotic membrane water permeability. The specific contribution of the CaSR signaling in this inhibitory process was assessed by using the CaSR allosteric modulator NPS-R568, which is known to be a specific and potent agonist of CaSR (Nemeth et al., 1996). Interestingly, CaSR activation per se induced a significant reduction of the basal AQP2-pS256 levels in HEK-293 cells, thus having an opposite effect with respect to vasopressin action. These data were also confirmed in HEK-293 cells transfected with two gain-of-function variants of CaSR used to mimic 'tonic' activation of CaSR. Given that, under basal conditions, NPS-R568 did not significantly alter the cAMP-dependent PKA activity, one possible explanation of this result is that CaSR activation reduces basal AQP2-pS256 levels as a consequence of the activation of the Ca^{2+}-regulated protein phosphatase 2A (PP2A), which is known to dephosphorylate AQP2-pS256 (Tamma et al., 2014b). Consistent with this hypothesis, we observed a tendency of a more pronounced reduction in AQP2-pS256 levels in cells expressing gain-of-function variants, which is in line with our previous data in HEK-293 cells demonstrating that two distinct activating CaSR variants were able to promote significantly higher Ca^{2+} release from the ER with respect to CaSR-wt-expressing cells (Ranieri et al., 2013). By contrast, we found that activation of CaSR signaling did not affect the basal levels of AQP2-pS261, meaning that modulation of AQP2 phosphorylation at S256 is the primary target through which CaSR signaling modulates the regulation of AQP2 trafficking and function.

Next, we proved, both in cells and in microdissected mouse collecting duct, that CaSR signaling elicits a negative feedback on cAMP-induced AQP2-pS256 phosphorylation and trafficking with the physiological consequence of reducing the osmotic water permeability response. In HEK-293 cells, activation of CaSR

Journal of Cell Science (2015) 128, 2350-2360 doi:10.1242/jcs.168096

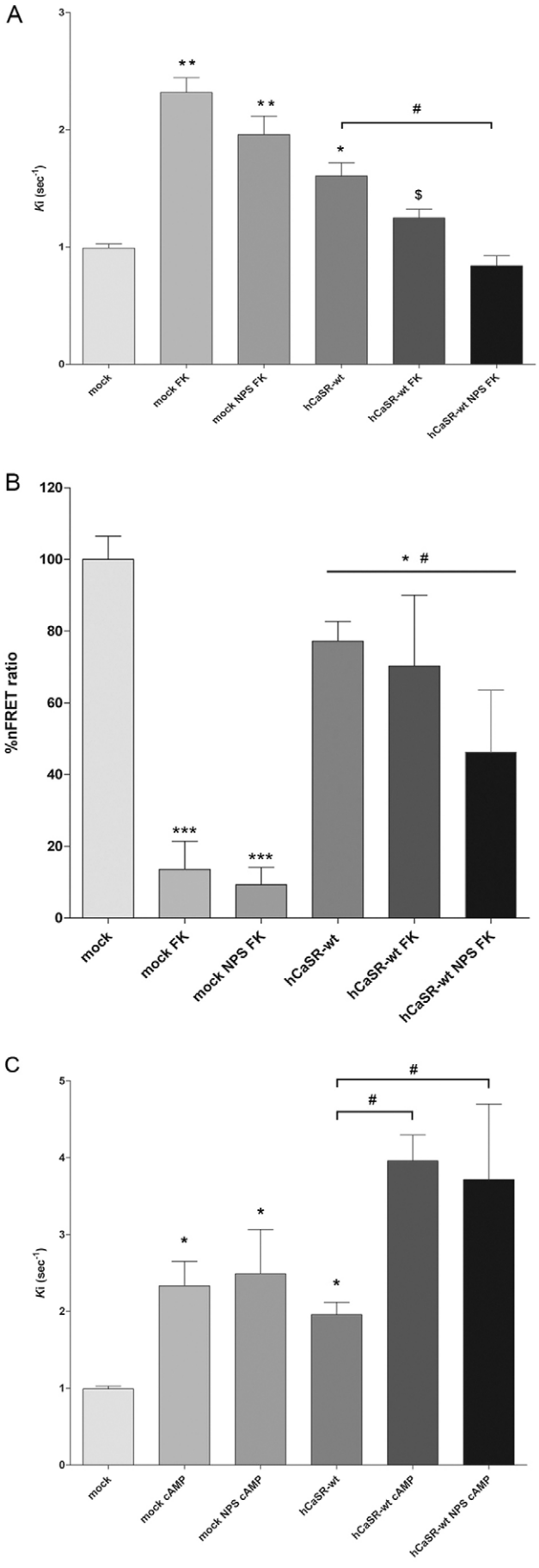

Fig. 5. CaSR signaling impairs the osmotic water permeability through inhibition of adenylate cyclase. (A) Effect of NPS-R568 and forskolin on AQP2-mediated water permeability. HEK-293 cells were loaded with Calcein Red-Orange AM for functional assays as described in Materials and Methods. In mock cells stably expressing AQP2 but not human (h)CaSR-wt, forskolin stimulation induced a significantly higher temporal osmotic response (reported as K_i, $^{**}P<0.0001$) which was not affected by NPS-R568 (NPS) (A). In contrast, in cells expressing CaSR-wt the increase in temporal osmotic response K_i was prevented. Moreover, when forskolin (FK) stimulation was performed in the presence of NPS-R568, the response was significantly reduced with respect to forskolin action alone (mean±s.e.m.; $^{*}P<0.01$ versus mock; $^{\#}P<0.05$ versus CaSR-wt; $^{\$}P<0.001$ versus mock with forskolin). (B) Evaluation of PKA activity by FRET analysis. Histogram compares changes in the nFRET ratio, among mock and cells expressing CaSR-wt, treated with forskolin (FK) and/or NPS-R568. In mock cells expressing AQP2 and not CaSR, forskolin stimulation caused a significant increase in PKA activity (reflected by a decrease in nFRET signal) and NPS-R568 had no effect. In contrast, CaSR-wt-expressing cells had a higher basal PKA activity and stimulation with forskolin failed to further activate PKA compared to mock cells (mean±s.e.m.; $^{*}P<0.01$ versus mock; $^{\#}P<0.01$ versus mock with forskolin). (C) Effect of NPS-R568 and 8-Br-cAMP (cAMP) on AQP2-mediated water permeability. Mock cells (not expressing CaSR and expressing AQP2) and CaSR-wt-expressing cells were treated with 8-Br-cAMP in the absence or in the presence of NPS-R568. 8-Br-cAMP stimulation resulted in a significant increase in the osmotic water permeability regardless of NPS-R568 treatment in mock and in CaSR-wt-expressing cells indicating that CaSR signaling exerts its inhibitory action mostly by reducing the activity of adenylate cyclase (mean±s.e.m.; $^{*}P<0.01$ versus mock; $^{\#}P<0.001$ versus CaSR-wt).

signaling prevented the increase in AQP2-pS256 induced by forskolin and abolished the increase in the osmotic water permeability. Measurements of PKA activity by FRET indicated that CaSR associated signaling causes a strong reduction in PKA activation in response to forskolin. Inhibition of cAMP accumulation can result from a Ca^{2+}-sensitive adenylate cyclase inhibition and/or phosphodiesterase activation.

Our data showing that the cell permeable cAMP analog 8-Br-cAMP causes a significant increase in the osmotic water permeability (regardless of NPS-R568 treatment in mock and in CaSR-wt-expressing cells), whereas forskolin stimulation results instead in a significant decrease in the osmotic water permeability under NPS-R568 treatment, indicate that CaSR signaling acts mostly by decreasing adenylate cyclase activity. In the collecting duct, the Ca^{2+}-inhibitable adenylate cyclase 6 (AC6, also known as ADCY6) regulates renal water excretion through control of vasopressin-stimulated cAMP accumulation (Rieg et al., 2010). AC6 is inhibited by Ca^{2+} at the micromolar level (Cooper et al., 1994) and is relatively abundant in collecting duct principal cells (Chabardes et al., 1996; Helies-Toussaint et al., 2000). Although both AC3 (also known as ADCY3) and AC6 are expressed in principal cells and have both been suggested to contribute to the overall rise in cAMP during vasopressin stimulation (Hoffert et al., 2005), the relevance of AC6 as a major enzyme in modulating the vasopressin-regulated water reabsorption is supported by the observation that collecting-duct-specific knockout of AC6 causes a urinary concentration defect associated with reduced vasopressin-stimulated cAMP accumulation (Roos et al., 2012). Taken together, our results indicate that the reduction in cAMP accumulation upon simultaneous stimulation with forskolin and activation of CaSR results from impairment of cAMP synthesis that is likely due to the inhibition of AC6 activity as a consequence of intracellular Ca^{2+} rise. Nevertheless cAMP hydrolysis by the Ca^{2+}/calmodulin-dependent PDE1 activity might also contribute to inhibition of cAMP content in response to forskolin (Bender and Beavo, 2006).

Note, however, that, in cells expressing wt-CaSR, the effect of forskolin stimulation on AQP2-pS256 levels was also impaired in

Journal of Cell Science (2015) 128, 2350-2360 doi:10.1242/jcs.168096

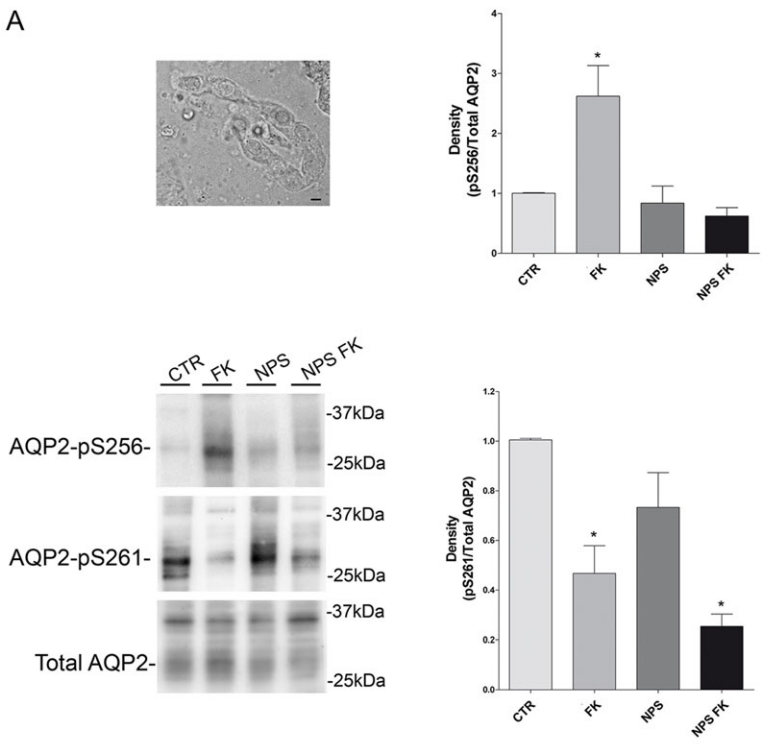

Fig. 6. CaSR signaling affects AQP2 localization and phosphorylation at S256. (A) Effect of NPS-R568 and forskolin on AQP2 AQP2-pS256 and AQP2-pS261 in microdissected mouse collecting duct tubules. Phase-contrast micrograph of microdissected mouse papillary collecting duct tubule (taken at 40× magnification, scale bar: 5µm). Mice renal tubules were isolated and treated as described in the Materials and Methods section. Total lysates were subjected to immunoblotting for total AQP2, AQP2-pS256 and AQP2-pS261. NPS-R568 (NPS) abolished the forskolin (FK)-dependent increase in AQP2-pS256. No effect of NPS-R568 on the forskolin induced decrease in AQP2-pS261 was observed. Signals were semiquantified by densitometry (mean±s.e.m.; **P*<0.05 versus CTR). (B) Immunofluorescence localization of AQP2 in mouse kidney slices (taken at 60× magnification, scale bars: 5µm). Under control conditions (CTR), AQP2 localized intracellularly. Forskolin stimulation caused a clear relocation of AQP2 on the apical plasma membrane. In contrast, exposure to NPS-R568 during forskolin stimulation prevented AQP2 redistribution and AQP2 had a prevalent intracellular distribution (NPS FK). NPS-R568 alone had no effect on basal AQP2 localization.

the absence of NPS-R568, as compared to mock cells not expressing CaSR. This indicates that the sole expression of CaSR in HEK-293 cells is able to attenuate the forskolin effect on cAMP levels and in turn on AQP2-pS256 phosphorylation. The possible explanation for this result might rely on our recent finding showing that CaSR expression in HEK-293 cells results in a significant reduction in basal intracellular Ca^{2+} levels compared to mock cells (Ranieri et al., 2013). Therefore, because vasopressin (and forskolin) stimulation causes Ca^{2+} mobilization from ryanodine-sensitive stores (Chou et al., 2000), more Ca^{2+} is released from intracellular stores in response to forskolin when CaSR is expressed, leading to a more pronounced inhibition of AC6 and/or activation of the PDE1 with the overall effect to reduce both cAMP and AQP2-pS256 levels. The activation of CaSR with NPS-R568 at the same time as forskolin stimulation will have the same effect because of Ca^{2+} release from intracellular stores. Nevertheless, it appears clear from functional studies, that the osmotic water permeability is reduced in HEK-293 cells expressing CaSR (and not in mock cells not expressing CaSR) in response to forskolin. The relevance of the CaSR signaling in regulating the water permeability in renal cells through regulation of AQP2 phosphorylation at S256 is underscored by the observation that the sole activation of CaSR with NPS-R568 reduces the basal osmotic water permeability.

The physiological relevance of all these observations obtained *in vitro* was confirmed in mouse and rat inner medulla. Experiments conducted in dissected mouse collecting duct suspensions were in good agreement with the data obtained in transfected cells. Stimulation with forskolin in the presence of the allosteric modulator completely prevented forskolin-induced increase in AQP2-pS256 and osmotic water permeability. Similar results were obtained in isolated rat kidney inner medulla. This is a particularly relevant result for two reasons: (1) the *ex vivo* experiments (evaluation of AQP2-pS256 levels and P_f in response to NPS-R568 and forskolin treatments) were conducted in dissected collecting ducts, thus after isolation of the nephron segment, where the expression of CaSR has been questioned by some authors (Loupy et al., 2012); and (2), in

Journal of Cell Science (2015) 128, 2350-2360 doi:10.1242/jcs.168096

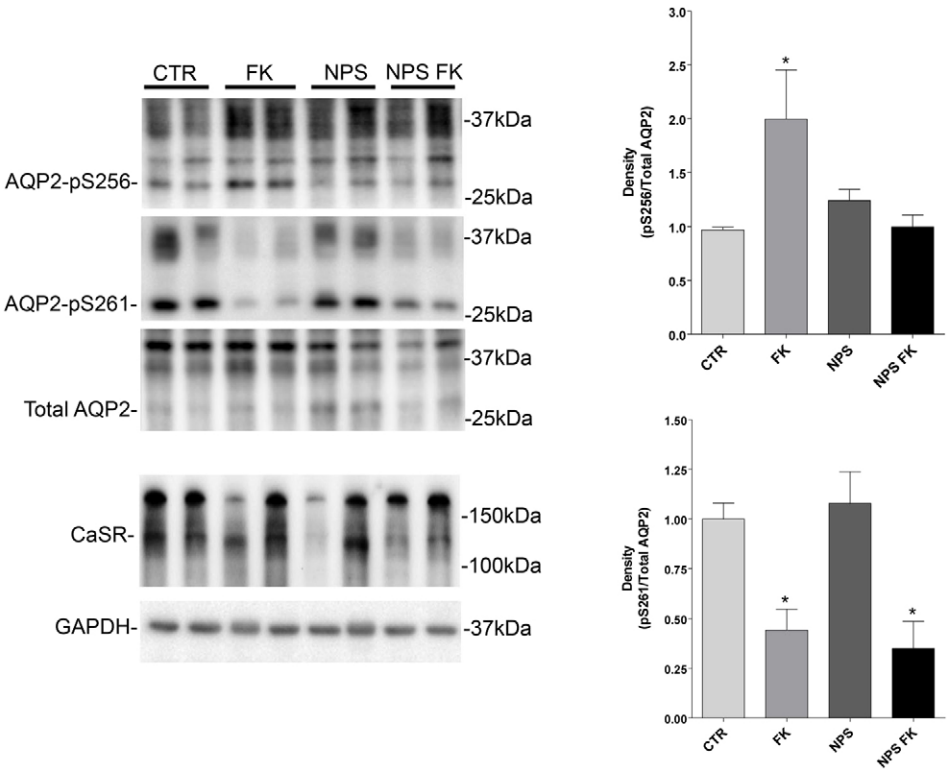

Fig. 7. Effect of NPS-R568 and forskolin on AQP2-pS256 and AQP2-pS261 in rat kidney slides. Rat kidney slices were treated as described in the Materials and Methods section. Total lysates were subjected to immunoblotting for total AQP2, AQP2-pS256 and AQP2-pS261. NPS-R568 (NPS) abolished the forskolin (FK)-dependent increase in S256 phosphorylation. No effect of NPS-R568 on the forskolin-induced decrease in AQP2-pS261 was observed. Signals were semi-quantified by densitometry (mean±s.e.m.; *P<0.05 versus CTR). CaSR expression in total lysates was confirmed using specific anti-CaSR antibodies.

dissected collecting ducts the CaSR was activated with the CaSR allosteric modulator NPS-R568 and its segment specific expression further confirmed by western blotting analysis and immunolocalization.

Although a previous study (Loupy et al., 2012) suggested that an extracellular cation-sensing G-protein-coupled receptor (GPRC6A) is also expressed in the collecting duct, it has to be underlined that GPRC6A and CaSR have very different affinities for extracellular Ca^{2+}, with CaSR being much more sensitive (more than one order) to the physiological agonist Ca^{2+} (Fenton et al., 2014) making CaSR the principal luminal receptor that senses amino acid and extracellular cations in the collecting duct.

Taken together, our data point to a crucial role of the CaSR expressed in the collecting duct in modulating AQP2 phosphorylation and trafficking and in turn water reabsorption. Here, we have dissected the mechanism by which CaSR acts on principal cells, showing that CaSR signaling results in a negative feedback on forskolin action (mimicking the vasopressin effect), primarily due to reduction of hormone-dependent cAMP generation and possibly hydrolysis. In particular, in principal cells, the co-expression of CaSR and the Ca^{2+}-inhibitable AC6 could be responsible for the negative regulation of the cAMP accumulation in the presence of high luminal Ca^{2+}, evoking intracellular Ca^{2+} release through CaSR activation.

In this respect is interesting to consider that CaSR and AC6 are co-expressed in the proximal tubule, in the cortical portion of the thick ascending limb and in the collecting duct, leading to the hypothesis that this confers high sensitivity to extracellular Ca^{2+} concentration to reduce the effects of distinct hormones selectively acting in those segments through the Gs–AC6–cAMP pathway, such as parathyroid hormone (in the proximal tubule) and vasopressin (in the thick ascending limb and collecting duct), respectively (Fenton et al., 2014; de Jesus Ferreira et al., 1998; Rieg et al., 2010). This conclusion is also supported by previous results demonstrating that extracellular Ca^{2+} inhibited hormone-dependent cAMP accumulation in the rat cortical thick ascending limb (de Jesus Ferreira et al., 1998).

To conclude, in the kidney collecting duct, the present data *in vitro* and in microdissected collecting ducts show that the inhibition of forskolin-stimulated cAMP accumulation is sensitive to variation of luminal Ca^{2+} allowing the modulation of AQP2-pS256 phosphorylation, trafficking and water transport. We propose that, as the luminal Ca^{2+} concentration becomes higher under vasopressin action, the strong inhibition of cAMP generation associated with CaSR activation can be a potent factor to reduce AQP2-mediated water reabsorption and reduce the risk of Ca^{2+} saturation. By extension, our data suggest, as an the emerging concept, that, within the nephron, co-expression of CaSR and AC6 elicits a negative feedback on hormones acting through the Gs–AC6–cAMP pathway, conferring high sensitivity of hormone effects to the extracellular Ca^{2+} concentration.

Table 1. Effect of NPS-R568 and forskolin on osmotic water permeability evaluated by stopped-flow light scattering

Condition	P_f (μm×s^{-1})	n	P
Control	359.6±48.2	4	
Forskolin	546.7±22.5*	4	0.02 (versus control)
NPS-R568	393.4±58.4	4	
NPS-R568+forskolin	307.2±68.5*	4	0.03 (versus forskolin)

The significant increase in P_f of the vesicles from isolated collecting ducts exposed to forskolin was prevented under CaSR activation with NPS-R568 and was not significantly different from the P_f measured in control vesicles. No significant effect of NPS-R258 alone on P_f was observed. Values are mean±s.e.m. (n=4). *P≤0.05.

MATERIALS AND METHODS

Materials

All chemicals were purchased from Sigma (Sigma-Aldrich, Milan, Italy). NPS-R568 was a kind gift from Amgen (Amgen Dompé Spa, Milan, Italy).

Journal of Cell Science

Journal of Cell Science (2015) 128, 2350-2360 doi:10.1242/jcs.168096

Calcein Red-Orange AM was obtained from Life Techonologies (Monza, Italy). Forskolin was purchased from Fermentek (Jerusalem, Israel). Vinpocetine was purchased from Tocris (Milan, Italy). The PP2A activity kit was purchased from Millipore (Millipore Corporation, USA).

Antibodies

Monoclonal CaSR antibody recognizing amino acids 15–29 at the extracellular N-terminus was from Sigma-Aldrich, Milan, Italy. Monoclonal antibody against glyceraldehyde-3-phosphate dehydrogenase (GAPDH, clone 6C5) was purchased from Millipore (Millipore Corporation, USA). To detect the total amount of AQP2, we used antibodies against the 20 amino-acid residue segment just N-terminal from the poly-phosphorylated region of rat AQP2 (CLKGLEPDTDWEEREVRRRQ) (Hoffert et al., 2006; Tamma et al., 2011). AQP2-pS256 antibodies were a kind gift from Peter Deen (Department of Physiology, Radboud University Medical Center, Nijmegen, The Netherlands) and has been described previously (Trimpert et al., 2012). AQP2-pS261 antibodies were purchased from Novus Biological (DBA, Milan, Italy). Secondary goat-anti-rabbit-IgG and anti-mouse-IgG antibodies conjugated to Alexa Fluor 488 were from Molecular Probes, Eugene, OR.

DNA constructs

For generation of the PCR3.1 constructs encoding for human wild-type CaSR (CaSR-wt) and its variants (CaSR-R990G; CaSR-N124K), the coding sequences were amplified by PCR and subcloned in frame in pAC-GFP1-N1. The obtained GFP-fused mutants are functional and correctly targeted to the plasma membrane. The presence of the GFP tag does not alter CaSR function and trafficking as previously described (Gama and Breitwieser, 1998).

Cell culture and transfection

Human embryonic kidney (HEK)-293 cells, were grown in Dulbecco's modified Eagle's medium (DMEM) with high glucose, GlutaMAX™, pyruvate and supplemented with 10% (v/v) fetal bovine serum and 100 i.u./ml penicillin and 100 mg/ml streptomycin at 37°C in 5% CO_2. The final Ca^{2+} concentration in the DMEM was 1.8 mM. HEK-293 cells were seeded on a poly-L-lysine hydrobromide substrate and grown for 24 h at 80% confluence. Cells were transiently transfected with plasmids (0.4 µg of DNA/cm^2) encoding for CaSR-wt and its variants fused with GFP, using lipofectamine (1 mg/ml) according to the protocol provided by the manufacturer (Life Technologies, Monza, Italy). Experiments were performed 48–72 h post-transfection.

Cell preparations

HEK-293 cells were transfected as described above and 48 h after transfection left in the basal condition or stimulated with NPS-R568 10 µM for 30 min in DMEM. Cells were lysed in RIPA buffer (150 mM NaCl, 10 mM Tris-HCl pH 7.2, 0.1% SDS, 1.0% Triton X-100, 1% deoxycholate and 5 mM EDTA) in the presence of proteases (1 mM PMSF, 2 mg/ml leupeptin and 2 mg/ml pepstatin A) and phosphatases (10 mM NaF and 1 mM sodium orthovanadate) inhibitors. Cellular debris was removed by centrifugation at 12,000 ***g*** for 10 min at 4°C. The supernatants were collected and used for the western blotting analyses. Alternatively, cells were scraped and sonicated in a buffer containing 220 mM mannitol, 70 mM sucrose and 20 mM Tris-HCl pH 7.4 in the presence of protease and phosphatase inhibitors. Nuclei- and mitochondria-enriched fractions were removed by centrifugation at 800 ***g*** and 8000 ***g***, respectively, for 20 min at 4°C. Membrane enriched fractions were obtained by centrifugation for 1 h at 4°C at 17,000 ***g***.

Dissection of mouse inner medullary collecting ducts

All animal experiments were performed according to approved guidelines. Inner medullary collecting ducts were dissected from mouse kidney as previously described (Tamma et al., 2005). Briefly, kidney papillae were rapidly minced and digested in a buffer that contained 118 mM NaCl, 16 mM HEPES, 17 mM Na-HEPES, 14 mM glucose, 3.2 mM KCl, 2.5 mM $CaCl_2$, 1.8 mM $MgSO_4$ and 1.8 mM KH_2PO4 (pH 7.4) in the presence of 0.2% collagenase and 0.2% hyaluronidase at 37°C for 90 min. After 45 min of incubation, 0.001% DNase I was added. The suspension was then was centrifuged at 200 ***g*** for 8 min to obtain tubular element of papilla. The obtained tubules then were treated for 45 min with 100 µM forskolin, 10 µM NPS-R568 or 100 µM forskolin and 10 µM NPS-R. Tubules were sonicated at 70 Hz for 15 s on ice-cold buffer in the presence of protease and phosphatase inhibitors. Samples were then centrifuged at 12,000 ***g*** for 10 min at 4°C and the supernatants used for western blotting analysis.

Kidney slices from rat inner medullary collecting ducts

Rat kidney slides from rat papilla were prepared as described (Boone et al., 2011). Briefly, Wistar Kyoto rats were anesthetized and killed by decapitation. Kidneys were quickly removed, and sections of ~0.5 mm were made and divided in four groups. Sectioned kidney papillae were equilibrated for 10 min in a buffer containing 118 mM NaCl, 16 mM Hepes, 17 mM Na-Hepes, 14 mM glucose, 3.2 mM KCl, 2.5 mM $CaCl_2$, 1.8 mM $MgSO_4$, and 1.8 mM KH_2PO_4 (pH 7.4). Subsequently kidney slices were left in the same buffer at 37°C or incubated with 10 µM forskolin, in the presence or in the absence of 10 µM NPS-R568 for 45 min or 5 mM Ca^{2+}. The treated sections were then homogenized with a mini-potter on ice-cold buffer containing 220 mM mannitol, 70 mM sucrose, 5 mM EGTA and 1 mM EDTA, 20 mM Tris-HCl pH 7.4, and protease and phosphatase inhibitors. Suspensions were then centrifuged at 12,000 ***g*** for 10 min at 4°C and the supernatants used for western blotting analysis.

Gel electrophoresis and western blotting

Proteins were separated on 8% or 13% bis-tris acrylamide gels under reducing conditions. Protein bands were electrophoretically transferred onto Immobilon-P membranes (Millipore Corporate Headquarters, Billerica, USA) for western blot analysis, blocked in TBS-Tween-20 containing 3% BSA and incubated with primary antibodies overnight. Immunoreactive bands were detected with secondary antibodies conjugated to horseradish peroxidase (HRP) obtained from Santa Cruz Biotechnologies (Tebu Bio, Milan, Italy). Membranes were developed using SuperSignal West Pico Chemiluminescent Substrate (Pierce, Rockford, USA) with Chemidoc System (Bio-Rad Laboratories, Milan, Italy). Band intensities were quantified by densitometric analysis using National Institutes of Health (NIH) ImageJ software.

Immunolocalization in kidney tissue slices

For immunolocalization of AQP2 in mouse kidney slides (250 µm), tissues were incubated at 37°C for 15 min in kidney slices buffer only. After equilibration, the slices were distributed into a multiwell plate containing either kidney slices buffer or 100 µM forskolin or 10 µM NPS-R or 100 µM forskolin and 10 µM NPS-R568.

After 35 min of incubation at 37°C, slices were fixed by immersion in 4% paraformaldehyde in phosphate-buffered saline (PBS) at 4°C overnight. The slices were then rinsed several times in PBS before use for immunostaining. Then, nonspecific binding sites were blocked with 1% bovine serum albumin in PBS (saturation buffer) overnight at 4°C.

Sections were then incubated with AQP2 antibodies (affinity purified; 1:3000 dilution) in saturation buffer overnight at 4°C. After washing in PBS, sections were incubated with secondary donkey-anti-rabbit-IgG conjugated to Alexa Fluor 488 (Life Technologies) for 2 h at room temperature. After washing in PBS, sections were mounted onto glass slides with Mowiol. Images were obtained with a confocal laser-scanning fluorescence microscope (Leica TCS SP2, Mannheim, Germany).

Water permeability video imaging measurements

Osmotic water permeability was measured by video imaging experiments. HEK-293 cells were grown on 40-mm-diameter glass coverslips and loaded with 20 µM of the membrane permeable dye Calcein Red-Orange AM for 45 min at 37°C and under 5% CO_2 in DMEM. Cells were left under basal condition or stimulated with NPS-R568 (10 µM) or forskolin (10 µM) for 30 min. The coverslips with dye-loaded cells were mounted in a perfusion chamber (FCS2 Closed Chamber System, BIOPTECHS, Butler, USA) and measurements were performed using an inverted microscope (Nikon Eclipse

TE2000-S microscope) equipped for single cell fluorescence measurements and imaging analysis. The sample was illuminated through a 40× oil immersion objective (NA 1.30). The sample loaded with Calcein Red-Orange AM was excited at 577 nm. Emitted fluorescence was passed through a dichroic mirror, filtered at 590 nm (Omega Optical, Brattleboro, VT, USA) and captured by a cooled ECCD camera (CoolSNAP HQ, Photometrics). Fluorescence measurements, following addition of isoosmotic (140 mM NaCl, 5 mM KCl, 1 mM $MgCl_2$, 1.8 mM $CaCl_2$, 10 mM Hepes, 5 mM Glucosio) or hyperosmotic (isoosmotic solution added with 100 mM Mannitol) solutions, were carried out using Metafluor software (Molecular Devices, MDS Analytical Technologies, Toronto, Canada). The time course of cell shrinkage was measured as a time constant (K_i, s^{-1}), a parameter directly correlated to membrane water permeability.

Preparation of membrane vesicles and stopped-flow light scattering analysis of membrane water permeability

The inner medulla from mouse kidney slices were homogenized manually with a mini-potter in ice-cold buffer containing 220 mM mannitol, 70 mM sucrose, 5 mM EGTA and 1 mM EDTA, 20 mM Tris-HCl, pH 7.4. Nuclei- and mitochondria-enriched fractions were removed by centrifugation at 800 ***g*** and 8000 ***g*** for 10 min, respectively. A plasma-membrane-enriched fraction was then obtained by centrifugation at 21,000 ***g*** for 1 h at 4°C. The pellet was gently resuspended in homogenization buffer, creating plasma membrane vesicles. The size of vesicles was determined with an N5 Submicron Particle Size Analyzer (Beckman Coulter Inc., Palo Alto, CA).

Osmotic water permeability of the plasma membrane vesicles was determined by stopped-flow light scattering, as described previously (Calamita et al., 2008). Briefly, the time course of vesicle volume change was followed from changes in intensity of scattered light at the wavelength of 450 nm using a BioLogic SFM-20 stopped-flow reaction analyzer (BioLogic, Claix, France) having a 1.6 ms dead time and 99% mixing efficiency in <1 ms. The sample temperature was kept at 20°C by a circulating water bath. Aliquots of vesicles were diluted into a hypotonic (220 mOsm) isolation medium (124 mM mannitol, 70 mM sucrose, 1 mM EDTA and 5 mM EGTA, 20 mM Tris-HCl pH 7.4). One of the syringes of the stopped-flow apparatus was filled with the vesicle suspension, whereas the other was filled with the same buffer to which mannitol was added to reach a final osmolarity of 500 mOsm to establish a hypertonic gradient (140 mOsm) upon mixing. The final protein concentration after mixing was 100 µg/ml. Immediately after applying a hypertonic gradient, water outflow occurs and the vesicles shrink, causing an increase in scattered light intensity. The data were fit to a single exponential function and the related rate constant (K_i, s^{-1}) of water efflux was determined. The osmotic water permeability coefficient (P_f), an index reflecting the osmotic water permeability of the vesicular membranes, was deduced using the equation:

$$P_f = K_i \cdot V_0 / A_v \cdot V_w \cdot \Delta C,$$

where K_i is the fitted exponential rate constant, V_0 is the initial mean vesicle volume determined as above, A_v is the mean vesicle surface, V_w is the molar volume of water and ΔC is the osmotic gradient. The medium osmolarity was verified by a vapor-pressure osmometer (Wescor Inc., Logan, UT).

FRET measurements

FRET experiments were performed as previously described (Henn et al., 2004; Tamma et al., 2007). Briefly, HEK cells were transiently co-transfected with plasmids encoding the regulatory and the catalytic subunit of PKA fused to cyan fluorescent protein (RII–ECFP) and yellow fluorescent protein (C–EYFP), respectively, and with plasmids encoding human CaSR wild-type (CaSR-wt) and its variants (CaSR-R990G; CaSR-N124K) (2.6 µg per each DNA) using the Lipofectemine protocol. RII–ECFP and C–EYFP have been previously described (Zaccolo and Pozzan, 2002) and were kindly provided by Manuela Zaccolo Department of Physiology, Anatomy and Genetics, University of Oxford, UK). After treatment of cells with NPS-R568 (10 µM) or forskolin (10 µM) for 30 min or with both NPS-R568 and forskolin, FRET measurements were carried out using MetaMorph software (Molecular Devices, MDS Analytical Technologies, Toronto, Canada). ECFP and EYFP were excited at 430 or 512 nm, respectively; fluorescence emitted from ECFP and EYFP was measured at 480/30 and 545/35 nm, respectively. FRET from ECFP to EYFP was determined by excitation of ECFP and measurement of fluorescence emitted from EYFP. Corrected nFRET values were determined according to Ritter et al. (2003).

Statistical analysis

Data are reported as mean±s.e.m. Statistical analysis was performed by one-way ANOVA followed by Newman–Keuls Multiple Comparison test with $P<0.05$ were considered statistically different.

Acknowledgements

We thank Amgen for providing the NPS-R568. We thank Patrizia Gena for her technical assistance in the stopped-flow light scattering experiments.

Competing interests

The authors declare no competing or financial interests.

Author contributions

M.R. and G.T. designed and performed the experiments, analyzed the data and contributed to the conceptual framework. A.D., A.R. and M.C. performed the experiments, analyzed the data, made illustrations and generated figures. M.S. read the manuscript and provided critical comments. G.C. provided expertise with stopped flow light scattering and experimental design. G.V. designed the experiments and wrote the manuscript.

Funding

This study was funded by Telethon [grant number GGP13227 to G.V.]; by a grant from University of Bari, Italy (Idea Giovani 2011 to G.T.); by a Research Program of National Interest (PRIN) project [grant number 01373409 to G.T.]; and by the Italian Space Agency (ASI) [grant number 2013-091-R.0 to G.V.].

Supplementary material

Supplementary material available online at
http://jcs.biologists.org/lookup/suppl/doi:10.1242/jcs.168096/-/DC1

References

Bender, A. T. and Beavo, J. A. (2006). Cyclic nucleotide phosphodiesterases: molecular regulation to clinical use. *Pharmacol. Rev.* **58**, 488-520.

Boone, M., Kortenoeven, M. L. A., Robben, J. H., Tamma, G. and Deen, P. M. T. (2011). Counteracting vasopressin-mediated water reabsorption by ATP, dopamine, and phorbol esters: mechanisms of action. *Am. J. Physiol. Renal Physiol.* **300**, F761-F771.

Brown, E. M. (1999). Physiology and pathophysiology of the extracellular calcium-sensing receptor. *Am. J. Med.* **106**, 238-253.

Bustamante, M., Hasler, U., Leroy, V., de Seigneux, S., Dimitrov, M., Mordasini, D., Rousselot, M., Martin, P.-Y. and Feraille, E. (2008). Calcium-sensing receptor attenuates AVP-induced aquaporin-2 expression via a calmodulin-dependent mechanism. *J. Am. Soc. Nephrol.* **19**, 109-116.

Calamita, G., Ferri, D., Gena, P., Carreras, F. I., Liquori, G. E., Portincasa, P., Marinelli, R. A. and Svelto, M. (2008). Altered expression and distribution of aquaporin-9 in the liver of rat with obstructive extrahepatic cholestasis. *Am. J. Physiol. Gastrointest. Liver Physiol.* **295**, G682-G690.

Chabardes, D., Firsov, D., Aarab, L., Clabecq, A., Bellanger, A.-C., Siaume-Perez, S. and Elalouf, J.-M. (1996). Localization of mRNAs encoding Ca2+-inhibitable adenylyl cyclases along the renal tubule: functional consequences for regulation of the cAMP content. *J. Biol. Chem.* **271**, 19264-19271.

Chou, C.-L., Yip, K.-P., Michea, L., Kador, K., Ferraris, J. D., Wade, J. B. and Knepper, M. A. (2000). Regulation of aquaporin-2 trafficking by vasopressin in the renal collecting duct: roles of ryanodine-sensitive Ca2+ stores and calmodulin. *J. Biol. Chem.* **275**, 36839-36846.

Cooper, D. M., Yoshimura, M., Zhang, Y., Chiono, M. and Mahey, R. (1994). Capacitative Ca2+ entry regulates Ca(2+)-sensitive adenylyl cyclases. *Biochem. J.* **297**, 437-440.

de Jesus Ferreira, M. C., Helies-Toussaint, C., Imbert-Teboul, M., Bailly, C., Verbavatz, J.-M., Bellanger, A.-C. and Chabardes, D. (1998). Co-expression of a Ca2+-inhibitable adenylyl cyclase and of a Ca2+-sensing receptor in the cortical thick ascending limb cell of the rat kidney: inhibition of hormone-dependent cAMP accumulation by extracellular Ca2+. *J. Biol. Chem.* **273**, 15192-15202.

Fenton, R. A., Murray, F., Dominguez Rieg, J. A., Tang, T., Levi, M. and Rieg, T. (2014). Renal phosphate wasting in the absence of adenylyl cyclase 6. *J. Am. Soc. Nephrol.* **25**, 2822-2834.

Gama, L. and Breitwieser, G. E. (1998). A carboxyl-terminal domain controls the cooperativity for extracellular Ca2+ activation of the human calcium sensing

receptor: a study with receptor-green fluorescent protein fusions. *J. Biol. Chem.* **273**, 29712-29718.

Helies-Toussaint, C., Aarab, L., Gasc, J. M., Verbavatz, J. M. and Chabardes, D. (2000). Cellular localization of type 5 and type 6 ACs in collecting duct and regulation of cAMP synthesis. *Am. J. Physiol. Renal Physiol.* **279**, F185-F194.

Henn, V., Edemir, B., Stefan, E., Wiesner, B., Lorenz, D., Theilig, F., Schmitt, R., Vossebein, L., Tamma, G., Beyermann, M. et al. (2004). Identification of a novel A-kinase anchoring protein 18 isoform and evidence for its role in the vasopressin-induced aquaporin-2 shuttle in renal principal cells. *J. Biol. Chem.* **279**, 26654-26665.

Hoffert, J. D., Chou, C.-L., Fenton, R. A. and Knepper, M. A. (2005). Calmodulin is required for vasopressin-stimulated increase in cyclic AMP production in inner medullary collecting duct. *J. Biol. Chem.* **280**, 13624-13630.

Hoffert, J. D., Pisitkun, T., Wang, G., Shen, R.-F. and Knepper, M. A. (2006). Quantitative phosphoproteomics of vasopressin-sensitive renal cells: regulation of aquaporin-2 phosphorylation at two sites. *Proc. Natl. Acad. Sci. USA* **103**, 7159-7164.

Loupy, A., Ramakrishnan, S. K., Wootla, B., Chambrey, R., de la Faille, R., Bourgeois, S., Bruneval, P., Mandet, C., Christensen, E. I., Faure, H. et al. (2012). PTH-independent regulation of blood calcium concentration by the calcium-sensing receptor. *J. Clin. Invest.* **122**, 3355-3367.

Nedvetsky, P. I., Tamma, G., Beulshausen, S., Valenti, G., Rosenthal, W. and Klussmann, E. (2009). Regulation of aquaporin-2 trafficking. *Handb. Exp. Pharmacol.* **190**, 133-157.

Nemeth, E. F., Steffey, M. E. and Fox, J. (1996). The parathyroid calcium receptor: a novel therapeutic target for treating hyperparathyroidism. *Pediatr. Nephrol.* **10**, 275-279.

Nemeth, E. F., Steffey, M. E., Hammerland, L. G., Hung, B. C. P., Van Wagenen, B. C., DelMar, E. G. and Balandrin, M. F. (1998). Calcimimetics with potent and selective activity on the parathyroid calcium receptor. *Proc. Natl. Acad. Sci. USA* **95**, 4040-4045.

Procino, G., Carmosino, M., Tamma, G., Gouraud, S., Laera, A., Riccardi, D., Svelto, M. and Valenti, G. (2004). Extracellular calcium antagonizes forskolin-induced aquaporin 2 trafficking in collecting duct cells. *Kidney Int.* **66**, 2245-2255.

Procino, G., Mastrofrancesco, L., Mira, A., Tamma, G., Carmosino, M., Emma, F., Svelto, M. and Valenti, G. (2008). Aquaporin 2 and apical calcium-sensing receptor: new players in polyuric disorders associated with hypercalciuria. *Semin. Nephrol.* **28**, 297-305.

Procino, G., Mastrofrancesco, L., Tamma, G., Lasorsa, D. R., Ranieri, M., Stringini, G., Emma, F., Svelto, M. and Valenti, G. (2012). Calcium-sensing receptor and aquaporin 2 interplay in hypercalciuria-associated renal concentrating defect in humans. An in vivo and in vitro study. *PLoS ONE* **7**, e33145.

Puliyanda, D. P., Ward, D. T., Baum, M. A., Hammond, T. G. and Harris, H. W.Jr. (2003). Calpain-mediated AQP2 proteolysis in inner medullary collecting duct. *Biochem. Biophys. Res. Commun.* **303**, 52-58.

Ranieri, M., Tamma, G., Di Mise, A., Vezzoli, G., Soldati, L., Svelto, M. and Valenti, G. (2013). Excessive signal transduction of gain-of-function variants of the calcium-sensing receptor (CaSR) are associated with increased ER to cytosol calcium gradient. *PLoS ONE* **8**, e79113.

Riccardi, D. and Brown, E. M. (2010). Physiology and pathophysiology of the calcium-sensing receptor in the kidney. *Am. J. Physiol. Renal Physiol.* **298**, F485-F499.

Rieg, T., Tang, T., Murray, F., Schroth, J., Insel, P. A., Fenton, R. A., Hammond, H. K. and Vallon, V. (2010). Adenylate cyclase 6 determines cAMP formation and aquaporin-2 phosphorylation and trafficking in inner medulla. *J. Am. Soc. Nephrol.* **21**, 2059-2068.

Ritter, M., Ravasio, A., Jakab, M., Chwatal, S., Furst, J., Laich, A., Gschwentner, M., Signorelli, S., Burtscher, C., Eichmuller, S. et al. (2003). Cell swelling stimulates cytosol to membrane transposition of ICln. *J. Biol. Chem.* **278**, 50163-50174.

Roos, K. P., Strait, K. A., Raphael, K. L., Blount, M. A. and Kohan, D. E. (2012). Collecting duct-specific knockout of adenylyl cyclase type VI causes a urinary concentration defect in mice. *Am. J. Physiol. Renal Physiol.* **302**, F78-F84.

Sands, J. M., Naruse, M., Baum, M., Jo, I., Hebert, S. C., Brown, E. M. and Harris, H. W. (1997). Apical extracellular calcium/polyvalent cation-sensing receptor regulates vasopressin-elicited water permeability in rat kidney inner medullary collecting duct. *J. Clin. Invest.* **99**, 1399-1405.

Sands, J. M., Flores, F. X., Kato, A., Baum, M. A., Brown, E. M., Ward, D. T., Hebert, S. C. and Harris, H. W. (1998). Vasopressin-elicited water and urea permeabilities are altered in IMCD in hypercalcemic rats. *Am. J. Physiol.* **274**, F978-F985.

Tamma, G., Carmosino, M., Svelto, M. and Valenti, G. (2005). Bradykinin signaling counteracts cAMP-elicited aquaporin 2 translocation in renal cells. *J. Am. Soc. Nephrol.* **16**, 2881-2889.

Tamma, G., Procino, G., Strafino, A., Bononi, E., Meyer, G., Paulmichl, M., Formoso, V., Svelto, M. and Valenti, G. (2007). Hypotonicity induces aquaporin-2 internalization and cytosol-to-membrane translocation of ICln in renal cells. *Endocrinology* **148**, 1118-1130.

Tamma, G., Lasorsa, D., Ranieri, M., Mastrofrancesco, L., Valenti, G. and Svelto, M. (2011). Integrin signaling modulates AQP2 trafficking via Arg-Gly-Asp (RGD) motif. *Cell. Physiol. Biochem.* **27**, 739-748.

Tamma, G., Di Mise, A., Ranieri, M., Svelto, M., Pisot, R., Bilancio, G., Cavallo, P., De Santo, N. G., Cirillo, M. and Valenti, G. (2014a). A decrease in aquaporin 2 excretion is associated with bed rest induced high calciuria. *J. Transl. Med.* **12**, 133.

Tamma, G., Lasorsa, D., Trimpert, C., Ranieri, M., Di Mise, A., Mola, M. G., Mastrofrancesco, L., Devuyst, O., Svelto, M., Deen, P. M. T. et al. (2014b). A protein kinase a-independent pathway controlling aquaporin 2 trafficking as a possible cause for the syndrome of inappropriate antidiuresis associated with polycystic kidney disease 1 haploinsufficiency. *J. Am. Soc. Nephrol.* **25**, 2241-2253.

Trimpert, C., van den Berg, D. T. M., Fenton, R. A., Klussmann, E. and Deen, P. M. T. (2012). Vasopressin increases S261 phosphorylation in AQP2-P262L, a mutant in recessive nephrogenic diabetes insipidus. *Nephrol. Dial. Transplant.* **27**, 4389-4397.

Valenti, G., Laera, A., Pace, G., Aceto, G., Lospalluti, M. L., Penza, R., Selvaggi, F. P., Chiozza, M. L. and Svelto, M. (2000). Urinary aquaporin 2 and calciuria correlate with the severity of enuresis in children. *J. Am. Soc. Nephrol.* **11**, 1873-1881.

Valenti, G., Laera, A., Gouraud, S., Pace, G., Aceto, G., Penza, R., Selvaggi, F. P. and Svelto, M. (2002). Low-calcium diet in hypercalciuric enuretic children restores AQP2 excretion and improves clinical symptoms. *Am. J. Physiol. Renal Physiol.* **283**, F895-F903.

Wilson, J. L. L., Miranda, C. A. and Knepper, M. A. (2013). Vasopressin and the regulation of aquaporin-2. *Clin. Exp. Nephrol.* **17**, 751-764.

Zaccolo, M. and Pozzan, T. (2002). Discrete microdomains with high concentration of cAMP in stimulated rat neonatal cardiac myocytes. *Science* **295**, 1711-1715.

Supplementary Data

Figure S1:

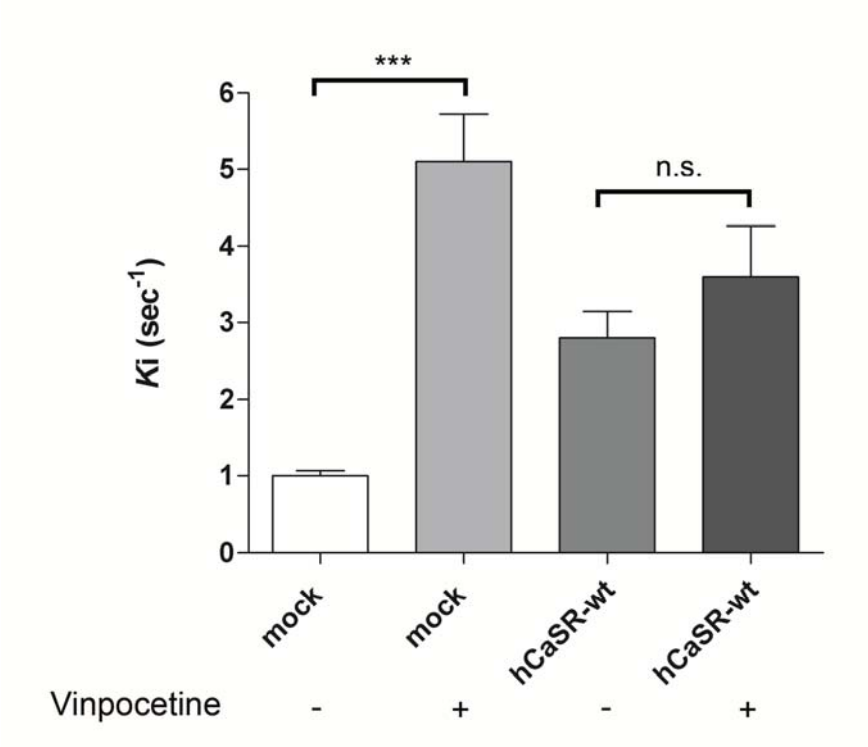

Effect of the selective PDE1 inhibitor vinpocetine, on osmotic water permeability. Mock HEK-293 cells or HEK-293 cells expressing hCaSR-wt were treated with 25 µM vinpocetine. In mock cells (expressing AQP2 and not CaSR) vinpocetine treatement induced a significantly higher temporal osmotic response (reported as K_i,). In contrast, no significant increase in osmotic response was observed in cells expressing the hCaSR-wt indicating that, at steady state, PDE1 inhibition (secondary to lower calcium levels in hCaSR-wt cells) can be responsible for the basal higher osmotic water permeability by increasing cAMP-dependent PKA activity at rest (Means ± SE; ***P<0.001 vs mock).

Figure S2:

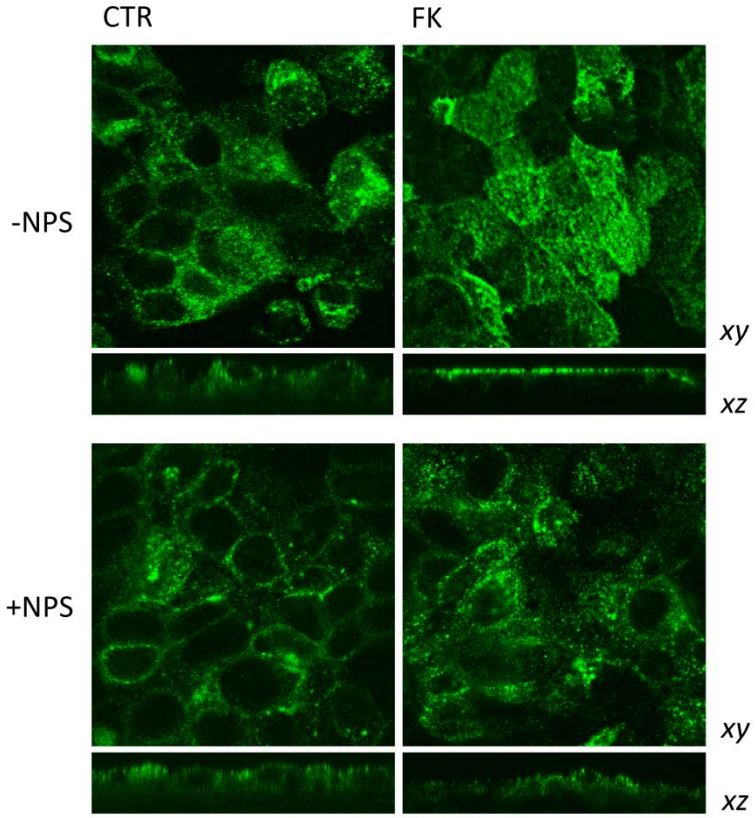

Immunofluorescence localization of AQP2 in mouse collecting duct cells (MCD4 cells) in response to FK in the presence of NPS-568. Under control condition (CTR) AQP2 localized intracellularly. FK stimulation caused a clear relocation of AQP2 on the apical plasma membrane (FK). In contrast, exposure to NPS-R568 during FK stimulation prevented AQP2 redistribution which had a prevalent intracellular distribution (NPS FK). Magnification: 60X.

Figure S3:

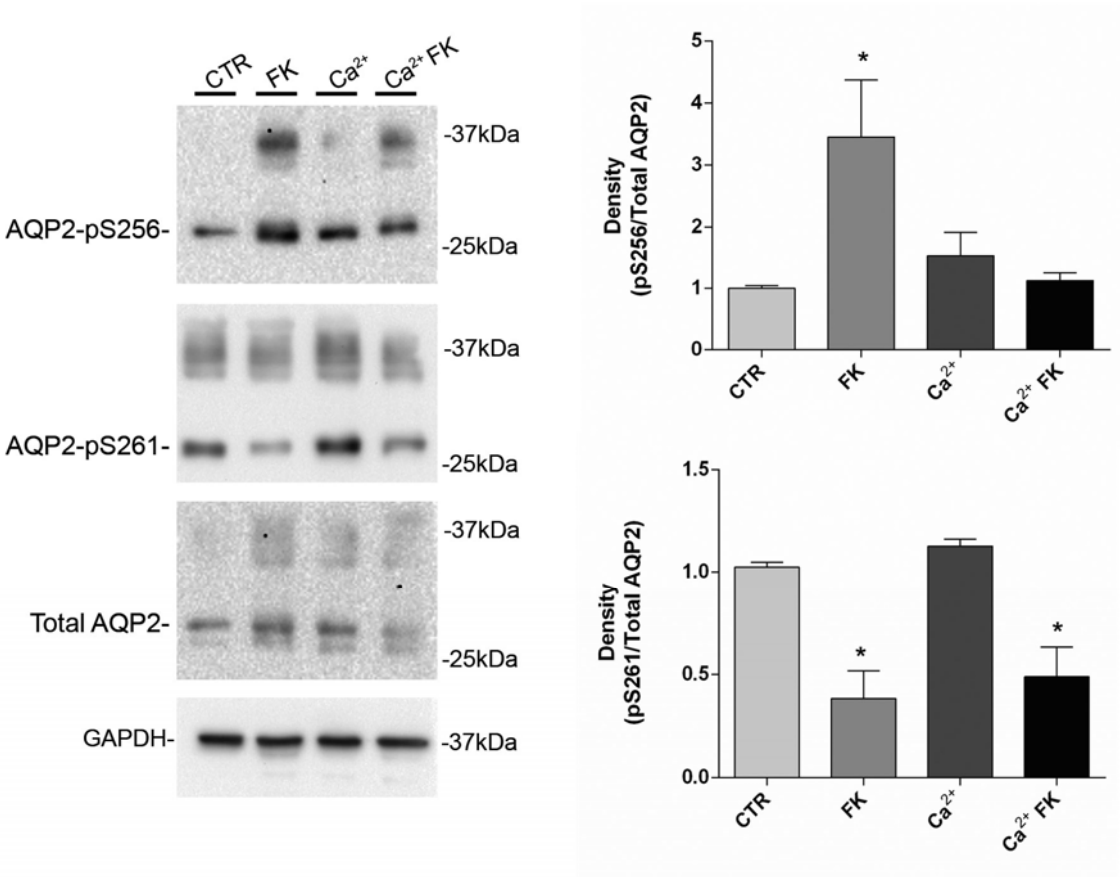

Effect forskolin stimulation on AQP2-pS256 and AQP2-pS261 in rat kidney slices exposed to in the presence of 5mM Ca2+. Rat kidney slices were stimulated with forskolin (FK) in the presence and in the absence of 5mM Ca2+ . Tissues were lysed, immunoblotted and probed with antibodies against total AQP2, AQP2-pS256 and AQP2-pS261. In the presence of 5mM Ca2+ , FK-dependent increase in S256 phosphorylation was prevented. No effect of 5mM Ca2+ on FK-induced decrease in AQP2-pS261 was observed. Signals were semi-quantified by densitometry (means ± SE; *P<0.01 vs CTR). CaSR expression in total lysates was confirmed using specific anti-CaSR antibodies (not shown).

Figure S4:

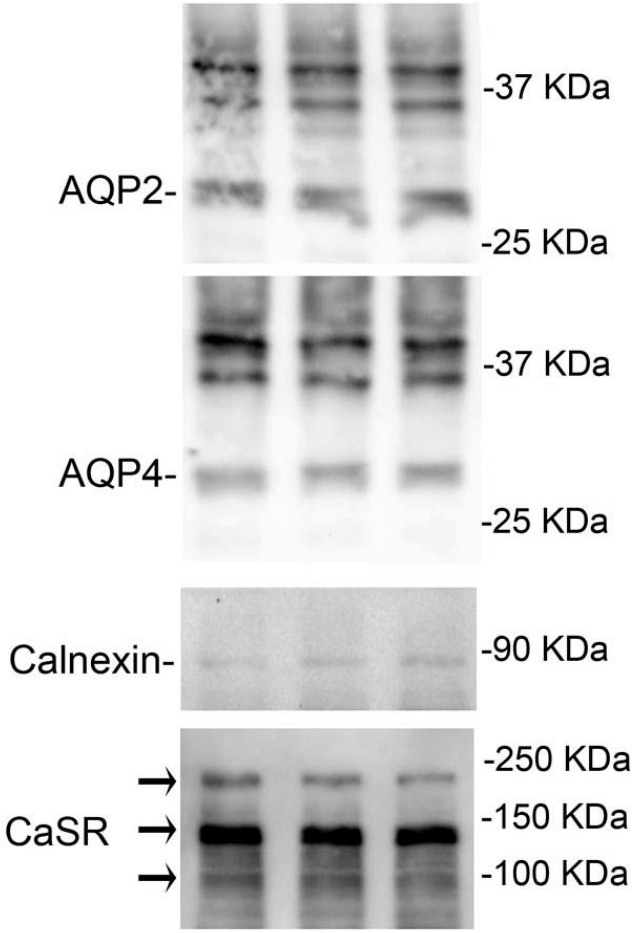

Biochemical characterization of renal vesicles isolated from mouse inner medulla. Mice inner medulla were isolated and treated as described under Materials and Methods. Lysates were blotted and probed for the expression of AQP2, AQP4, calnexin and CaSR.